A Study of the Fundamental Contributions to Line Edge Roughness in a 193 nm, Top Surface Imaging System

Mark H. Somervell
Department of Chemical Engineering, The University of Texas at Austin, Austin, TX 78731

David S. Fryer
Department of Chemical Engineering, The University of Wisconsin, Madison, Wisconsin 53706

Brian Osborn and Kyle Patterson
Department of Chemistry, The University of Texas at Austin, Austin, TX 78731

Jeffrey Byers
International SEMATECH, 2706 Montopolis Dr. Austin, TX 78741

C. Grant Willson
Department of Chemical Engineering, The University of Texas at Austin, Austin, TX 78731

Journal of Vacuum Science and TechnologyB

Abstract:

Top surface imaging systems based on vapor phase silylation have been investigated for use at a variety of wavelengths. This approach to generating high aspect ratio, high resolution images held great promise particularly for 193 nm and EUV lithography applications. Several 193 nm TSI systems have been described that produce very high resolution (low k factor) images with wide process latitude. However, because of the line edge roughness associated with the final images, TSI systems have fallen from favor. In fact, TSI does not appear in the strategy or plan for any imaging technology at this time.

Most of the 193 nm TSI systems that have been studied are based on poly(*p*-hydroxystyrene) resins. These polymers have an unfortunate combination of properties that limit their utility in this application. These limiting properties include 1) High optical density 2) Poor silylation contrast 3) Low glass transition temperature of the silylated material. These shortcomings are related to inherent polymer characteristics and are responsible for the pronounced line edge roughness in the poly(*p*-hydroxystyrene) systems. We have synthesized certain alicyclic polymers that have higher transparency and higher glass transition temperatures. Using these polymers, we have demonstrated the ability to print high resolution features with very smooth sidewalls. This paper describes the synthesis and characterization of the polymers, their application to top surface imaging at 193 nm, and the analysis that was used to tailor the processing and the polymer's physical properties to achieve optimum imaging.

Introduction

Top surface imaging (TSI) using vapor phase silylation has long been studied as an alternative to single layer imaging. Many imaging systems have been proposed that utilize this technology.[1-9] These processes were inspired by the early work of Taylor,[1-2] and they are reviewed in a book chapter by B.J Lin.[10] Past TSI systems have been described by a creative set of acronyms including DESIRE,[5-6] PRIME,[7] SUPER,[8] and SAHR.[9] Most of these processes have been tailored for 365 nm or 248 nm exposure, and some have been modified to work at shorter wavelengths.[11-12] TSI systems utilize different mechanisms for image development than traditional chemically amplified resists. In one of these schemes, the films are exposed under conditions in which they are very strongly absorbing and the exposure energy is deposited in the near surface volume of the resist film. The exposure typically causes a cross-linking reaction that may be achieved by one of several mechanisms. This local cross-linking reaction serves to densify the exposed volume of the resist and thereby modify (reduce) the permeability of the film in that region. The resist film is then exposed to a controlled pressure of a reactive amino-silane vapor that diffuses into the resist and

reacts with polar, protic sites in the polymer. A typical reaction of this sort is shown in Scheme A which shows the silylation of poly(*p*-hydroxystyrene) (PHOST) with dimethylsilyldimethylamine (DMSDMA).

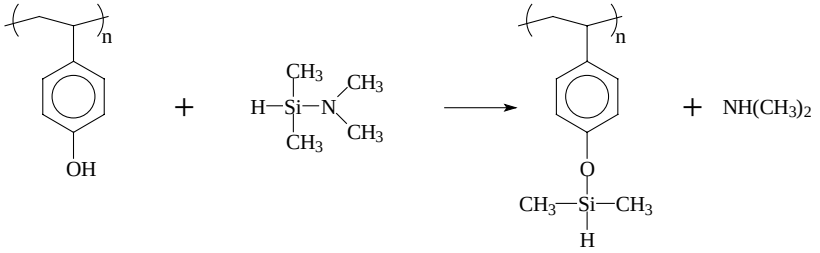

Scheme A

The silylating agent has a much lower diffusion rate into the cross-linked material, and therefore silylation occurs more slowly in the exposed areas. In principle, etching the silylated film in oxygen removes the cross-linked material while the silylated material is oxidized to a glass that serves as an etch barrier. This diffusion-based scheme leads to positive tone images.

There is a different approach to top surface imaging in which the silylation contrast is created by a photo-induced switch in chemical reactivity as shown in Figure 1.

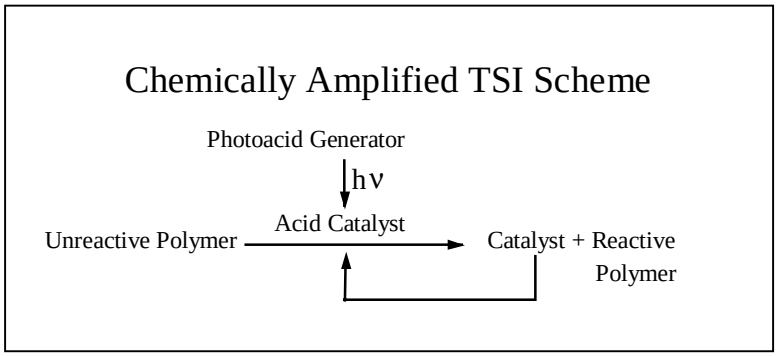

Figure 1: Schematic for using chemical reactivity as a silylation switch

A polymer that is unreactive to silylation is rendered reactive through a chemically amplified mechanism. Figure 2 shows how this process can be implemented in poly(*t*-BOC-styrene) (referred to as *t*-BOCPS).[3,4] This example serves to display some important features of the process design. In this system the polymer has two states, reactive and unreactive. Since the polymer is always in one of these two states, the silylation is digital. Several of the processes described above utilize photo-induced modulation of the silylating agent's transport into the film. All of the film is reactive, and while the exposure lessens the extent of reaction, it does not prevent it from occurring. In this sense, these systems are analog.

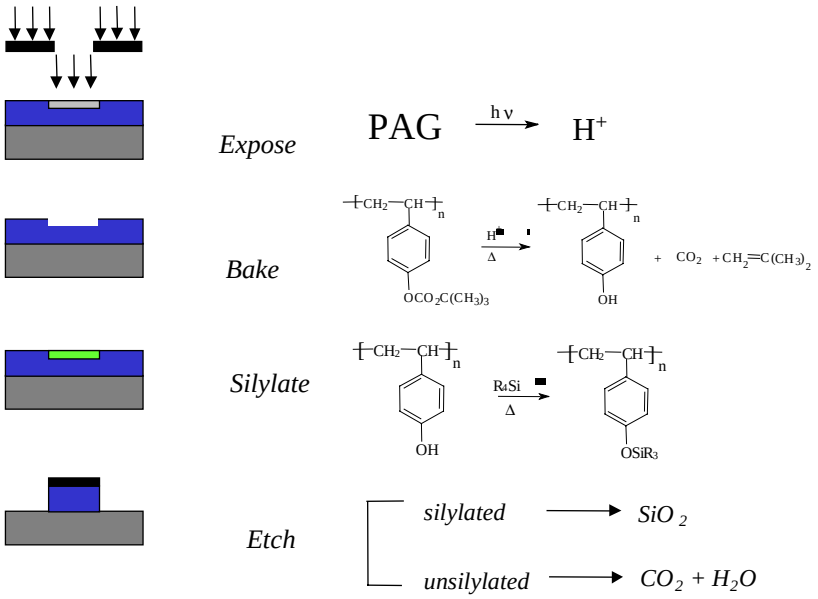

Figure 2: Schematic of Negative Tone TSI system

The other attribute of this system is subtle but important. The silylation reaction changes the mass and volume of the polymer substantially. Silylation of PHOST with DMSDMA as shown in Reaction Scheme A increases the polymer molecular weight by approximately thirty percent and the silylated regions must swell accordingly. This swelling results in image distortion. In the t-BOCPS system, exposure and baking causes deprotection (which changes the polymer's reactivity to silylation) with concurrent loss of volatile products. The film shrinks during the PEB as shown in Figure 2, but the silylation step swells the film. If the mass loss and mass gain are carefully balanced, the net volume change can be zero and the image distortion can be eliminated.[13] This system may therefore be described as a "digital, zero-volume change, TSI process."

Materials and Experimental

Experimental

Solvents for organic syntheses were obtained from Aldrich Chemical Company and used as received unless otherwise specified. ^{1}H-nuclear magnetic resonance spectra were taken on a General Electric QE-300 (300 MHz) NMR. Bulk T_g measurements were recorded with a Perkin Elmer Differential Scanning Calorimeter (scan rate 20° C/min). On-wafer T_g measurements were made with a scanning thermal microscope made by Topmetrix (Details of this measurement are provided in a publication by Fryer *et al.* [14]). Bulk infrared measurements were taken with a Nicolet Avatar 360 FTIR while on-wafer IR readings were taken using a Nicolet Magna FTIR. Polymer molecular weights were measured using a gel permeation chromatograph fitted with a refractive index detector made by Viscotek (molecular weights are based on poly(styrene) standards.)

The resists were coated with a FSI Polaris 2000 track. An ISI 193 nm microstepper with a numerical aperature of 0.6 and a partial coherence of 0.7 was used for exposures. A Genesis 200C silylation tool was used for silylation, and one of two different LAM TCP 9400 SE etchers was used to dry develop the images. Either a Hitachi 4400 or a Hitachi S 4500 was used to take scanning electron micrographs.

Decoration of silylated materials was performed in the following manner. After silylation was completed, the imaged fields were cleaved perpendicular to the imaged lines. The sample was then placed edge up in a Plasma Technology Oxford μ80 reactive ion etch chamber where it was etched for 25 seconds in an oxygen plasma. The etcher settings were 10 sccm of O_2, 30 mT pressure, and 45 W of power. (The conditions and

configuration of the etcher are such that horizontal etching is minimized.) After etching, samples were sputter-coated with gold/palladium and viewed on a scanning electron microscope.

Materials

This research has focused on two different polymer systems. The first is poly(t-BOC-styrene) (t-BOCPS), and the second is an alternating copolymer of sulfur dioxide and 5-(2-*t*-butoxycarbonyloxy-2-trifluoromethyl-3,3,3-trifluoropropyl)norbornene ($PFASO_2$).The structures of these materials are shown in Figure 3.

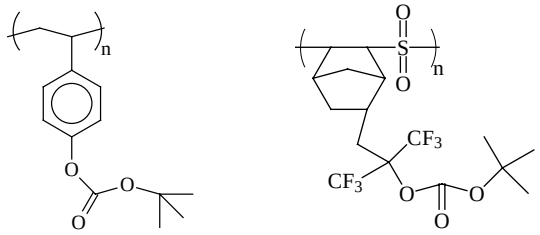

Figure 3: Structures of poly(t-BOC-styrene) and poly[5-(2-t-butoxycarbonyloxy-2-trifluoromethyl-3,3,3-trifluoropropyl)norbornene -alt-sulfur dioxide]

The t-BOCPS was prepared by polymerization of 4-t-butyloxycarbonyloxystyrene monomer donated by Triquest chemical company. A typical polymerization procedure is given below. t-BOC–styrene monomer, 20 g (0.091 mol), was placed in a round-bottom flask with 40 g of dry THF. The solution was heated to 60º C and then 0.2 g of AIBN was added. The resulting solution was stirred overnight, cooled to room temperature, and diluted with an additional 20 ml of THF. The THF solution was added to 1 L of rapidly-stirred methanol whereupon a white precipitate formed. The polymer was isolated by filtration, dried *in vacuo* at room temperature for 24 hours, redissolved in THF, and then reprecipitated. The resulting white polymer powder was obtained in 85 percent yield after the two precipitations and typically had a number average molecular weight of 25,000 with a M_w/M_n of 1.8. The $PFASO_2$ copolymer was synthesized in accordance with the procedure of Ito *et al.*[15]

Dimethylsilyldimethylamine was purchased from Silar Laboratories, and 1,2-dimethyldisilyldimethylamine was donated by Dr. David Wheeler from Sandia National Labs. The silylating agents were used as received.

Triphenyl sulfonium bromide was synthesized following the literature procedure by Hacker, *et al.*[16] Magnesium powder, 21 g, was suspended in 200 ml of CaH_2-dried diethyl ether in a 500 ml flask. The reaction was held at room temperature by cooling as 141 g bromobenzene was added slowly. After addition of the bromobenzene, the solution was stirred at room temperature for two hours. The ether was then removed *in vacuo*, leaving a dark, viscous oil. Benzene, 200 ml, was added with stirring, and removed again *in vacuo*. The addition of benzene and subsequent removal was repeated a total of three times to remove residual diethyl ether. Benzene, 150 ml, and n-heptane, 300 ml, were added with stirring. Diphenyl sulfoxide, 36 g, was dissolved in 100 ml of benzene and added dropwise to the refluxing mixture. When addition was complete, the mixture was refluxed for 48 hours. A slurry of 300 ml of 48% HBr and 300g crushed ice was slowly added to the cooled reaction mixture. The aqueous phase was separated, and the organic phase washed twice with 100 ml portions of 5% HBr. These combined aqueous extracts were extracted 4 times with 200 ml portions of dichloromethane. The combined organic phases were dried over $MgSO_4$ the solvent was removed *in vacuo* to leave a yellow residue which was dissolved in the minimum amount of dichloromethane and added to 250 ml diethyl ether to precipitate triphenylsulfonium bromide as a white powder. Yield=12.4g (20.3%) mp=284-287C (lit.=285-7° C [8])

Triphenylsulfonium nonaflate was prepared by metathesis. Potassium nonaflate, 6.6 g, and triphenylsulfonium bromide, 6.7 g, were partitioned between 30 ml nitromethane and 30 ml de-ionized water by vigorously stirring the two-phase mixture for one hour. The organic phase was then separated,

extracted three times with de-ionized water, and dried over $MgSO_4$. The solvent was removed *in vacuo* to give triphenylsulfonium nonaflate as an oily residue. Repeated washing of the organic residue with diethyl ether followed by solvent evaporation *in vacuo* removed residual nitromethane and left 7.92 g (yield=72%) of triphenylsulfonium nonaflate as a white crystalline solid. [mp=88-89º C, anal. calcd. for $C_{22}H_{15}F_9O_3S_2$: C, 46.98%; H, 2.69%; F, 30.40%; O, 8.53%; S, 11.40%. found C, 47.14%; H, 2.71%; F, 29.86%; O, 8.52% (by subtraction); S, 11.73%. ^{19}F NMR ($CDCl_3$, reference = $CFCl_3$, ppm): δ –80.8 (3F), -114.4 (2F), -121.1 (2F), -125.6 (2F)]

Results and Discussion

Imaging of t-BOCPS

The lithographic process scheme for imaging t-BOCPS is shown in Figure 2 above. The photoresist consisted of the t-BOCPS polymer, a triphenyl sulfonium nonaflate photoacid generator (PAG) at a loading of 4 weight percent to the polymer, tridodecyl amine (10 molar percent to the PAG), and 6 grams of propylene glycol methyl ether acetate (PGMEA) for every gram of t-BOCPS.

The photoresist was coated (PAB = 100° C for 60 seconds) to give a film thickness of approximately 650 nm. After coating, the wafer was exposed and then baked for 1 min at 90º C. The wafer was silylated with 30 Torr of 1,2-dimethyldisilyldimethylamine (DMDSDMA, see structure given in Figure 4) for 60 seconds at 90º C. This silylating agent was used for two reasons. First, because it has 2 silicon atoms, it forms an excellent etch barrier upon oxidation. Secondly, the amount of mass that this silylation agent appends to the polymer chain almost exactly balances the mass lost during the deprotection reaction. Finally, the wafer was etched using the LAM 9400 SE with a TCP power of 260 W, a bias power of 115 W, a gas flow of 60 sccm O_2, a pressure of 2.7 mT, and a chuck temperature of –42º C.

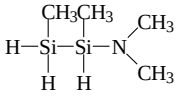

Figure 4: Structure of 1,2-Dimethyldisilyldimethylamine

Both isolated and nested features generated by this process are shown in Figures 5 and 6 respectively. The process provides high resolution, high aspect ratio images with straight sidewall angles, and the mask linearity for isolated and nested features is excellent as shown in Figure 7. Unfortunately, the isolated and nested lines are not sized at the same dose. However, the required dose for either feature type is quite low and shows that this system is capable of printing high resolution features at very low exposure doses.

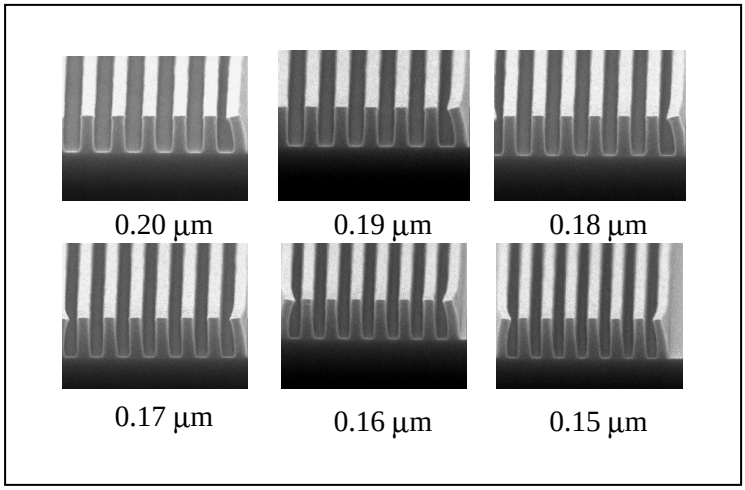

Figure 5: Nested lines printed with a binary mask at 3.8 mJ/cm^2

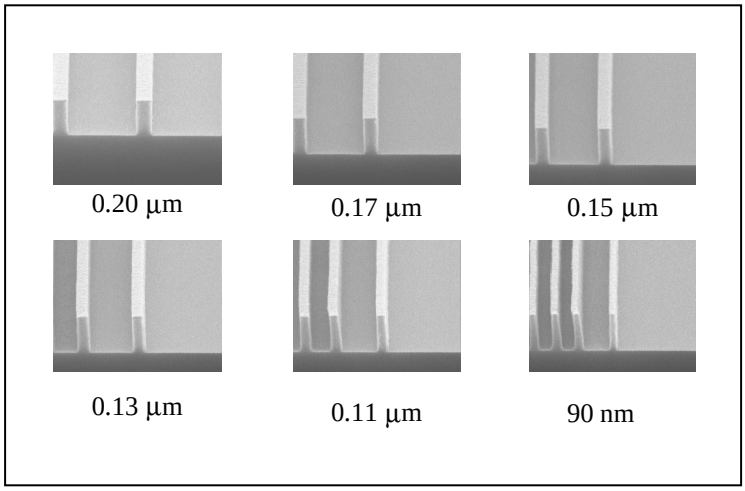

Figure 6: Isolated lines printed with a binary mask at 6.2 mJ/cm^2

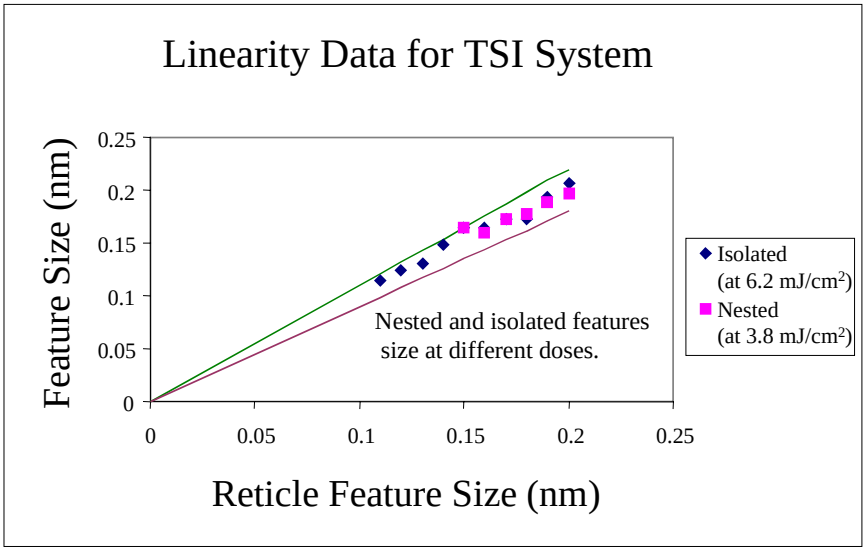

Figure 7: Linearity Data for t-BOCPS system

Many TSI systems have demonstrated the ability to resolve small features, but unfortunately, these features have always had rough sidewalls. This system exhibits the same problem. Figure 8 shows several high resolution SEM micrographs of the above structures and reveals the roughness of these features.

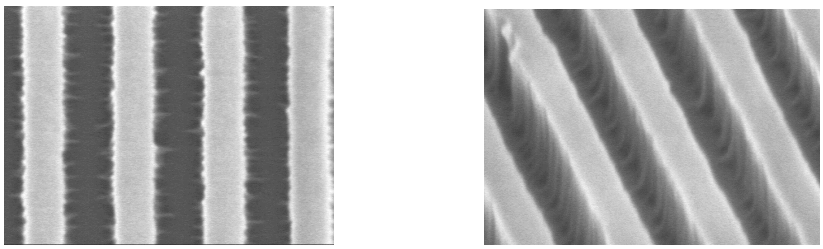

Figure 8: Top down and tilted views showing line edge roughness in TSI system

Although it is possible to print high resolution, high quality features with the t-BOCPS system, the roughness of the features prohibits their use in manufacturing.

Sources of Line Edge Roughness in t-BOCPS system

Several attempts were made to improve the line edge roughness (LER) in the t-BOCPS system. Literature dry development recipes that were reported to improve the LER in other TSI systems were employed.[17, 18] These procedures were not successful in the t-BOCPS system, however, and it continued to demonstrate a high degree of LER. Therefore an analysis of the fundamental characteristics of the t-BOCPS material itself was performed and several properties that contribute to line edge roughness were identified.

The first contributor is the high optical density of the t-BOCPS photoresist at 193 nm. The measured absorbance for t-BOCPS at 193 nm is 39 μm^{-1}; this absorbance is so high that the 1/*e* penetration depth is only 25 nm. This exceptionally high absorbance influences the shape of the isoenergy profiles in the resist film. Because the light intensity in the film decays exponentially, the energy is deposited into the photoresist in a shallow, bowl-shaped volume. A simulated cross section of the energy deposition profile in t-BOCPS is provided in Figure 9. Note that the energy decays to less than twenty percent of the incident intensity at a depth of 50 nm.

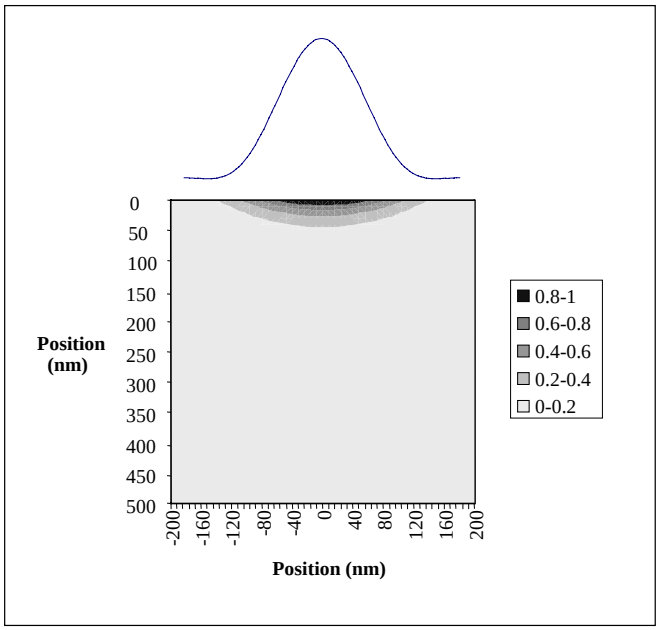

Figure 9: Aerial Image and Deposition of energy in opaque t-BOCPS material

The extent of silylation can be observed experimentally by cross-sectioning an exposed and silylated film and decorating the sample with a low-power oxygen plasma. Figure 10 shows a scanning electron micrograph of t-BOCPS exposed at 193 nm, silylated under conditions given earlier, and then decorated.

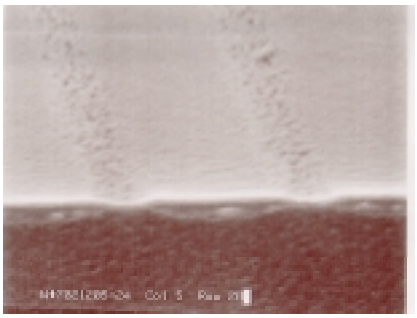

Figure 10: Silylation profile of t-BOCPS exposed with 193 nm light

This silylation profile is very like that of the simulated energy deposition profile shown in Figure 9. Such a cross-section can easily lead to line edge roughness because it comes to a sharp thin point at the edge of the feature. As the reactive ion etch proceeds, the very thin edge must serve as an etch mask, but because it lacks structural integrity, it erodes in a stochastic fashion along the full length of the line and generates a rough edge. This rough edge is then transferred down through the underlying resist during the etch and contributes to the roughness in the final images.

A second contribution to the line edge roughness is the silylation contrast of the system. The silylation contrast can be measured by exposing an array of open frames on a wafer and monitoring the chemical changes that occur through infrared spectroscopy. The degree of deprotection after post-exposure bake can be measured by observing the change in the carbonyl peak. Likewise, the extent of silylation can be monitored through the Si-H stretch that appears at 2100 cm^{-1}. (These experiments were performed using 248 nm illumination because the field size is large enough to interrogate with an infrared beam and the resist is transparent at this wavelength.) Figure 11 is a plot of the extent of silylation versus dose for a wafer silylated with 30 Torr of DMSDMA for 60 seconds at 90° C. The silylation response for an ideal lithographic system should be as close to a step function as possible. The threshold for silylation could then be tuned to correspond to the feature edge and the undesired exposure that occurs in the "dark" areas of the photoresist could be mitigated. Unfortunately, Figure 11 shows that the silylation response in this system is not a step function. The silylation contrast (measured by the slope of the line as the silylation begins) is more nearly linear than the dissolution response to dose that occurs in wet-developed systems. Since the silylation contrast is not very high, the edge of the silylated feature is somewhat indistinct due to the pseudo-Gaussian shape of the aerial image, and this "gray-scale" response manifests itself as line edge roughness in the final image.

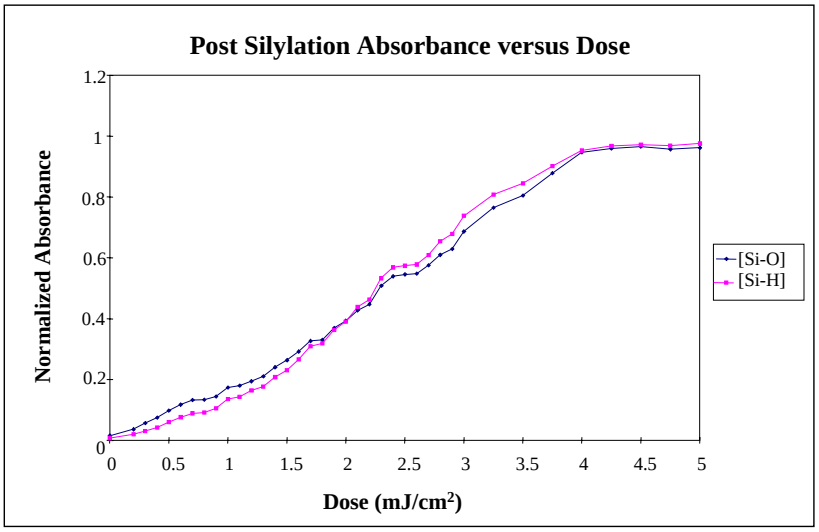

Figure 11: Silylation Contrast plot for t-BOCPS

The silylation response for an ideal lithographic system should be as close to a step function as possible. The threshold for silylation could then be tuned to correspond to the feature edge and the undesired exposure that occurs in the "dark" areas of the photoresist could be mitigated. Unfortunately, Figure 11 shows that the silylation response in this system is not a step function. The silylation contrast (measured by the slope of the line as the silylation begins) is more nearly linear than the dissolution response to dose that occurs in wet-developed systems. Since the silylation contrast is not very high, the edge of the silylated feature is somewhat indistinct due to the pseudo-Gaussian shape of the aerial image, and this "gray-scale" response manifests itself as line edge roughness in the final image.

The final contributing factor to the line edge roughness in the t-BOCPS system is the glass transition temperature (T_g) of the silylated polymer. Substituted PHOST polymers used in photoresist formulation generally have glass transition temperatures between 120°-180° C. However, when PHOST undergoes silylation, its T_g drops drastically. In the t-BOCPS system, varying types of PHOST copolymers are formed during the imaging and silylation process. First, the exposure and bake creates copolymers of the t-BOCPS and the PHOST itself. In regions of high exposure (i.e. at the center of the feature), the polymer is completely deprotected. Closer to the edges of the features, the light is less intense, and a smaller amount of deprotection occurs. In these regions, a PHOST/t-BOCPS copolymer is formed, and the ratio of the two depends on the intensity of exposure and the bake conditions. After silylation, the completely deprotected polymer in the center of the feature forms a completely silylated polymer, and copolymers of the t-BOC-protected PHOST and the silylated PHOST are formed toward the edge of the feature. All of these silylated polymers have lowered T_gs, and the completely silylated polymer has a T_g below the standard silylation temperature of 90° C.

In order to characterize how the T_g of the polymer depends on silylation, on-wafer glass transition temperature measurements were taken. Wafers coated with t-BOCPS were exposed with an array of open fields of varying dose. Using an IR beam, it was possible to monitor the deprotection in each field (and thus the copolymer ratio between protected and deprotected PHOST). Next, the wafers were silylated with DMSDMA for twenty minutes to ensure complete silylation. Finally, the T_g measurements were taken of various fields to document the glass transition temperature as a function of the extent of silylation. These data are shown in Figure 12.

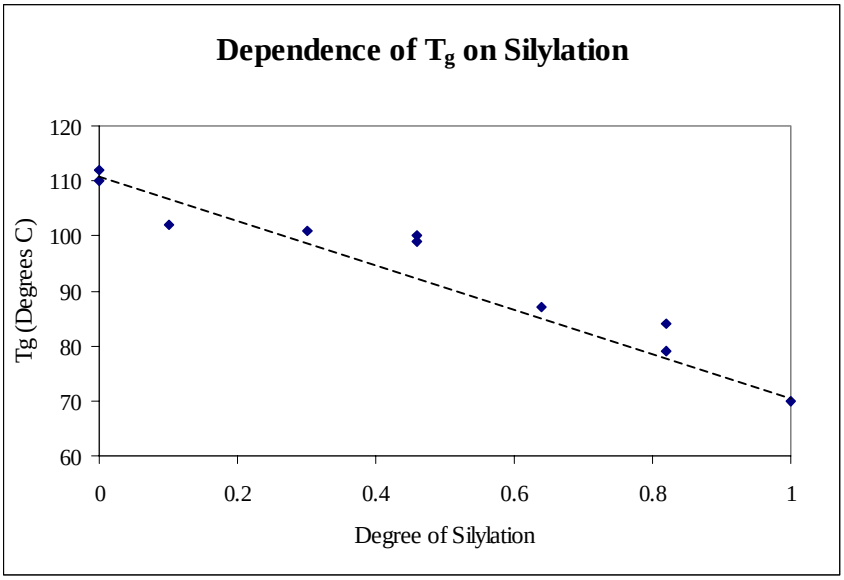

Figure 12: Glass transition temperature of silylated polymers (the line is drawn to guide the eye)

This figure shows that as the degree of silylation increases, the glass transition temperature of the t-BOCPS/silylated PHOST copolymer drastically decreases. In fact, at complete silylation, the glass transition temperature of the silylated polymer is 70° C. Therefore, it is not surprising that silylation temperatures in excess of 70° C would lead to problematic imaging. Figure 13 shows another silylation profile in which the silylation was conducted at 90° C and the silylated polymer started to flow. (This particular wafer was imaged with 248 nm light so that the whole bulk is silylated.)

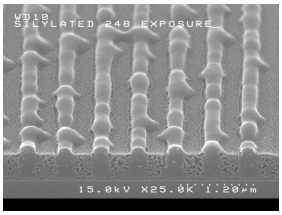

Figure 13: Flow of silylated material

This type of image flow is highly undesirable because the polymer is moving into the unexposed areas where there should be no silylation. Image distortion that results from the flow of the silylated polymer is translated to roughness after the etch.

The low T_g of the silylated material can also contribute to LER through a second physical mechanism. Recent work by Lin and coworkers demonstrates how phase incompatibility of the copolymers near the feature edge can lead to line edge roughness in bilayer resist systems.[19] It is quite likely that the silylated polymer is incompatible with the protected precursor. In the boundary area near the feature edge, there exists a range of compositions following silylation. This photogenerated blend of copolymers may be thermodynamically unstable with respect to phase separation, but below the T_g, the rate of separation is very slow. It is therefore important not to heat the sample to a temperature at which the rate of this phase separation is significant with respect to the processing time scale. Phase separation can generate aggregates of etch resistant material at the edge of the silylated profile and thereby introduce line edge roughness.

Imaging of $PFASO_2$

Since the advent of TSI, researchers have almost exclusively studied systems based on phenolic polymers. The problems that lead to line edge roughness in the t-BOCPS system are inherently tied to the properties of that polymeric material; so, it would appear that other platforms such as alicyclic polymers may be better suited for use as TSI resins. In general, these materials have high transparency at 193 nm and also have higher T_gs. Finding functional groups that will silylate under standard processing conditions is somewhat challenging. In the PHOST-based systems, acidic phenolic functionalities have been used as sites for silylation. Aliphatic alcohols on alicyclic backbones are not nearly as acidic as phenols and do not undergo silylation readily. Carboxylic acids have also been studied as silylatable functionalities. Although they undergo silylation quite readily, they also hydrolyze very quickly.[20] The hexafluoroisopropanol group (pictured in Figure 14) is as acidic as phenol[21] and can be attached to a more transparent alicyclic backbone.

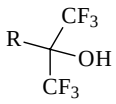

Figure 14: Hexafluoroisopropanol group

There is a report of an alternating copolymer of sulfur dioxide and 5-(2-*t*-butoxycarbonyloxy-2-trifluoromethyl-3,3,3-trifluoropropyl)norbornene.[15] This material was synthesized and auditioned as a new TSI platform. A photoresist was formulated with this polymer, triphenyl sulfonium nonaflate photoacid generator (4% by weight to polymer), and PGMEA. Films cast from this solution had an absorbance of only 1.7 μm^{-1} (base *e*) at 193 nm.

This resist formulation was evaluated to provide guidance in setting process conditions for the imaging experiments. In Figure 15 are a series of IR spectra that show the resist after casting, after exposure and bake, and after silylation. The resist was silylated with 45 torr of DMSDMA for 9 minutes at 90° C.

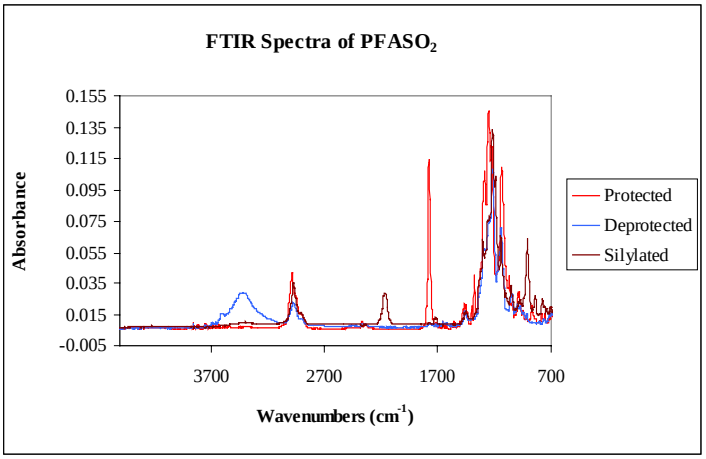

Figure 15: FTIR spectrum showing deprotection and silylation characteristics of $PFASO_2$

The cast polymer has a strong carbonyl peak at 1700 cm^{-1}. The spectrum for the deprotected polymer demonstrates the expected loss of carbonyl and the growth of an –OH stretch. Finally, the silylated polymer is characterized by the appearance of a peak at 2100 cm^{-1} which arises from the Si-H bond present in the polymer after silylation. These spectra show that the $PFASO_2$ copolymer undergoes the deprotection and silylation chemistry necessary to function as a TSI polymer.

The silylation contrast of this system was measured. The photoresist formulation detailed above was coated on a wafer and exposed with an array of open frames having varying doses. As before, the deprotection and silylation response was monitored with infrared spectroscopy. The silylation repsonse was measured as a function of silylation time for this new system, but the other silylation conditions were held constant at 45 Torr of DMSDMA and 90° C. Figure 16 shows of plot of the silylation response to increasing exposure dose.

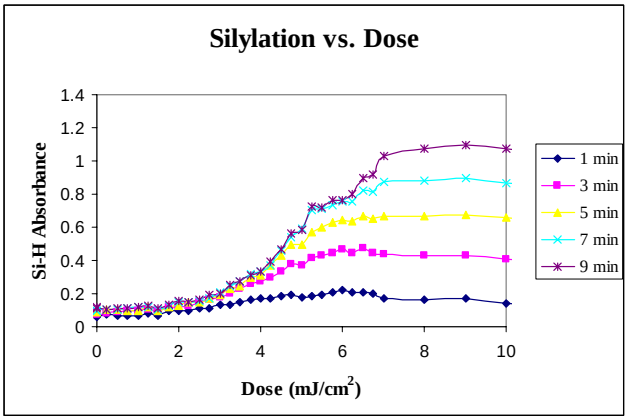

Figure 16: Silylation contrast curves for $PFASO_2$ at 90 °C

Again, the silylation response does not demonstrate ideal non-linearity. It appears that the contrast (as measured by the slope of the curve during the time which the silylation is "turning on") increases slightly with silylation time. More bulk silylation occurs for longer times because the silylating agent has more

time to penetrate into the resist film and reach unreacted sites. Although this experiment does not reveal the optimal silylation time for imaging, it definitely shows that silylation times longer than one minute are required to sufficiently silylate this material at this temperature and pressure of silylating agent.

Figure 17 shows a simulation of the energy deposited in a film with the transparency of $PFASO_2$ ($1.7\ \mu m^{-1}$) on top of an ideal ARC (analagous to Figure 9 for the t-BOCPS system).

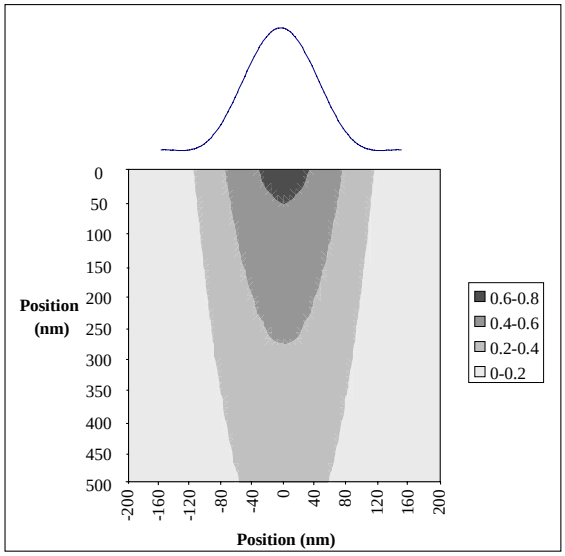

Figure 17: Aerial Image and Deposition of energy in transparent $PFASO_2$

Notice now that the light penetrates deeper into the film, and the shape of the iso-energy curves no longer has a sharp point at the feature edge. Decorated silylation profiles for this system were created. The SEM photo (see Figure 18) clearly demonstrates the expected improvement in silylation profile.

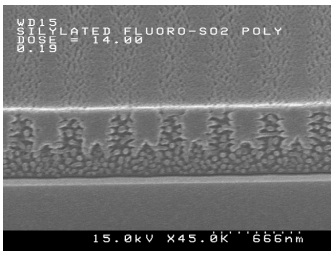

Figure 18: Silylation profiles in $PFASO_2$

Indeed the increased transparency leads to a more square silylation profile that provides a much more robust etch barrier for image transferal.

The next step in the material evaluation was to measure the T_g of the silylated material. A sample of the resist was coated and exposed so that the polymer was completely deprotected. The exposed sample was then reacted with 45 Torr of DMSDMA at 90° C for 2 hours. After this time, an IR spectrum was taken of the film and revealed that all alcohol groups in the polymer had been silylated. The sample's T_g was then measured three times and found to range from 105° C to 111° C. Therefore, the completely silylated $PFASO_2$ polymer has a T_g approximately 35° C higher than the completely silylated PHOST polymer in the t-BOCPS system. Since the T_g of the polymer is above the silylation temperature, the silylated polymer has no chance to flow, and the line edge integrity is maintained.

Finally, the polymer was imaged. The primary goal was to see if this resist system would yield smooth features. Therefore, in order to remove any standing wave effects, Shipley's XP 96585-G0 ARC with a thickness of 580 Å was first coated on silicon. The resist was then coated and baked at 90° C for 60s (thickness = 600 nm), exposed, baked at 90° C for 2 minutes, silylated with 45 Torr of DMDSDMA for 5 minutes at 90° C, and then dry developed (TCP power = 260 W, Bias = 75 W, Pressure = 2.7 mT, Flow = 60 sccm O_2, Chuck Temperature = -25° C). Figure 19 shows both top down and tilted cross sectional views of the structures printed at 18 mJ/cm^2.

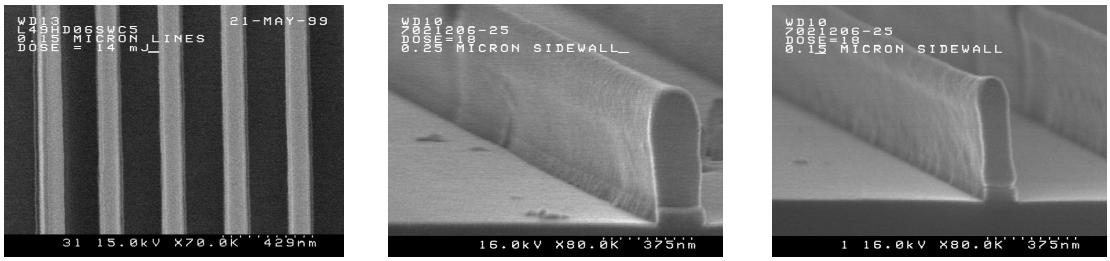

Figure 19: Top down view of 0.15 μm nested lines, side view of 0.25 μm isolated line, side view of 0.15 μm isolated line

These images show that it is indeed possible to print very smooth, high resolution features in this resist.

MIT Lincoln Labs has developed a protocol for measuring LER in TSI and other single layer resist systems.[22] The sample shown in Figure 19 was sent to them for analysis. A representative photo and data set is shown in Figure 20 and Table 1 respectively.

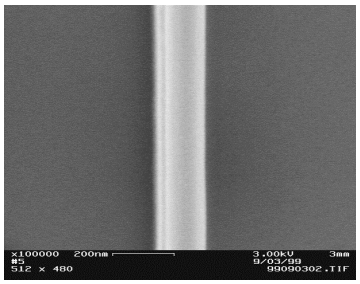

Figure 20: Top down SEM taken of imaged PFASO$_2$ at Lincoln Labs

Measurement	Width (nm)	Left Edge Sigma (nm)	Right Edge Sigma (nm)	Percentage
Type A	165.2	1.34	0.99	0.71
Type B	150.8	0.92	0.99	0.63

Table 1: Summary of line edge roughness data

The MIT protocol can use one of two algorithms for selecting the feature edges and making the LER measurements. Regardless of the algorithm used, the line edge roughness is less than one percent of the feature size. This more transparent polymer with a high glass transition temperature yields much smoother features than the t-BOCPS system. (Since the silylation contrast of the PFASO$_2$ system is similar to that of the t-BOCPS, its effect on the LER is not as significant as the optical density or the T_g of the silylated polymer.) In fact, the features printed in the PFASO$_2$ system are as smooth as any printed with a single layer resist system.

The MIT protocol can use one of two algorithms for selecting the feature edges and making the LER measurements. Regardless of the algorithm used, the line edge roughness is less than one percent of the feature size. This more transparent polymer with a high glass transition temperature yields much smoother features than the t-BOCPS system. (Since the silylation contrast of the PFASO$_2$ system is similar to that of

the t-BOCPS, its effect on the LER is not as significant as the optical density or the T_g of the silylated polymer.) In fact, the features printed in the $PFASO_2$ system are as smooth as any printed with a single layer resist system.

Conclusions

Most researchers have concluded that top surface imaging systems that involve vapor phase silylation inherently lead to features with rough sidewalls. This conclusion is not true. A digital, zero-volume change, TSI process has been developed. When applied to a PHOST-based system, this process provides very high resolution images with severe edge roughness. Changing to an alicyclic polymer platform with improved transparency, higher glass transition temperature, and a new silylatable functionality provided high resolution images with line edges as smooth as any wet-developed system. It is not yet clear exactly what level of absorbance is required to enable smooth features in TSI; the experiments described in this paper have essentially bounded the problem. It is clear, however, that TSI can tolerate higher optical densities than wet-developed systems and it is clear that this process has the potential for producing higher aspect ratio relief images than those that can be obtained by wet development. The exact transparency requirement of these systems is now being explored, but the results of this preliminary investigation clearly demonstrate that the new polymer platforms warrant further study for top surface imaging applications.

Acknowledgements

The authors would like to thank SEMATECH, IBM, David Wheeler, MIT Lincoln Labs, and Triquest Chemical Company for their contribution to this work. This material is based upon work supported under a National Science Foundation Graduate Fellowship and is also supported by the Semiconductor Research Consortium (Contract No. LC-460).

References

1) G. N. Taylor, L. E. Stillwagon, and T. Venkatesan, J. Electrochem. Soc. **131**, 1658 (1984).

2) T. M. Wolf, G. N. Taylor, T. Venkatesan, and R. T. Kretsch, J. Electrochem. Soc. **131**, 1664 (1984).

3) S. A. MacDonald, H. Schlosser, N. J. Clecak, C. G. Willson, and J. M. J. Fréchet, Chem. Mater. **4**, 1364 (1992).

4) H. Ito, S. A. MacDonald, R.D. Miller, and C. G. Willson, U.S. Patent 4,552,833 (1985).

5) F. Coopmans and B. Roland, Proc. SPIE **631**, 34 (1986).

6) F. Coopmans, Solid State Technol. **30(6)**, 93 (1987).

7) C. Pierrat, S. Tedesco, F. Vinet, M. Lerme, and V. Dal'Zotto, J. Vac. Sci Technol. B **7**, 1782 (1989).

8) C. M. J. Mutsaers, F. A. Vollenbroek, W. P. M. Nijssen, and R. J. Visser, Microelecro. Eng. **11**, 497 (1990).

9) E. K. Pavelchek, J. F. Bohland, J. W. Thackery, G. W. Orsula, S. K. Jones, B. W. Dudley, S. M. Bobbio, and P W. Freeman, J. Vac. Sci. Technol. B **8**, 1497 (1990).

10) B. J. Lin, in *Introduction to Microlithography*, ACS Symposium Series Vol. 219, edited by L. F. Thompson, C. G. Willson, and M. J. Bowden (American Chemical Society, Washington, D.C., 1983), p. 287-350.

11) S. C. Palmateer, R. R. Kunz, M. W. Horn, A. R. Forte, and M. Rothschild, Proc. SPIE **2438**; 455 (1994).

12) J. Hutchinson, V. Rao, G. Zhang, A. Pawloski, C. Fonseca, J. Chambers, S. Holl, S. Das, C. Henderson, and D. Wheeler, Proc. SPIE **3333**, 165, (1998).

13) S. V. Postnikov, M. H. Somervell, C. L. Henderson, C. G. Willson, S. Katz, J. Byers, A. Qin, and Q. Lin, Proc. SPIE **3333**, 997 (1998).

14) D. S. Fryer and J. J. dePablo, P. F. Nealey, Proc SPIE **3333,** 1031 (1998).

15) H. Ito, N. Seehof, R. Sato, T. Nakayama, and M. Ueda, in *Micro- and Nanopatterning Polymers*, ACS Symposium Series Vol. 706 (American Chemical Society: Washington D.C., 1998), pp. 210-212.

16) N. P. Hacker and J. L. Dektar, J. Am. Chem. Soc. **112**, 6004 (1990).

17) H. G. Kim, M. S. Kim, C. K. Bok, B. J. Park, J. W. Kim, K. H. Baik, and D. H. Lee, Proc SPIE **3333**, 554 (1998).

18) J. Vertommen, W. Klippert, A. M. Goethals, and F. Van Roey, J. Photopolym. Sci Technol. **11**, 597**.**

19) Q. Lin, R. Sooriyakumaran, and W. Huang, Proc. SPIE **3999** (2000).

20) N. M. Nobuyuki, S. Mori, T. Morisawa, Y. Kaimoto, M. Endo, T. Ohfuji, K. Kuhara, and M. Sasago, Proc. SPIE **3333**, 493 (1998).

21) J. R. Gandler and W. P. Jencks, J. Amer. Chem. Soc. **104**, 1937 (1982).

22) C. M. Nelson, S. Palmateer, and T. Lyszczarz, Proc. SPIE **3332**, 19 (1998).